

Cobalt in strontium titanate as a new off-center magnetic impurity

I. A. Sluchinskaya* and A. I. Lebedev
Moscow State University, Moscow, 119991 Russia
(Dated: October 28, 2021)

The local structure and oxidation state of the cobalt impurity in SrTiO₃ is studied by X-ray absorption fine structure (XAFS) spectroscopy. The synthesis conditions, under which cobalt predominantly (up to 76%) substitutes the atoms at the *A* site of the perovskite structure, is found for SrTiO₃(Co) samples. By varying the synthesis conditions, it is possible to appreciably change the ratio between the concentrations of cobalt atoms incorporated into the *A* and *B* sites. It is established that the oxidation state of cobalt is +2 at the *A* site and +3 at the *B* site. It is revealed that the Co impurity at the *A* site is off-center, and its displacement from the lattice site is ~ 1.0 Å. First-principles calculations show that an isolated Co³⁺ ion at the *B* site is diamagnetic, whereas the Co²⁺ ion at the *A* site is in a high-spin state ($S = 3/2$).

Physics of the Solid State 61, 390 (2019); DOI: 10.1134/S1063783419030302

I. INTRODUCTION

The search for new magnetic off-center impurities, which can simultaneously result in the appearance of ferroelectric and magnetic ordering and the magnetoelectric interaction in crystals [1], is currently a topical problem. The materials characterized by these properties are classified as multiferroics—multifunctional materials, which open new opportunities for modern electronics and spintronics.

It is obvious that to obtain multiferroic properties, a material must have a magnetic moment, e.g., as a result of its doping with magnetic impurities. The position of an impurity atom in a crystal and its local environment may have an appreciable effect on its magnetic moment. In addition, atoms of 3*d* transition elements can exist in several oxidation states, which depend on the position of an atom in a lattice, its local environment (isolated atom, complexes with different defects), and the presence of other donors and acceptors in samples.

The oxidation and spin states can be changed by varying the synthesis conditions. Thus, in the case of the Mn impurity in SrTiO₃, it was shown that the oxidation state and the ratio between the concentrations of atoms at different lattice sites can be changed by varying the annealing temperature and the stoichiometry of samples (see [2, 3] and the references therein). Our studies of nickel-doped strontium titanate showed that the magnetic state of nickel depends on what kind of impurity complexes are formed in the doping process. The magnetic moment of nickel in the Ni²⁺–V_O complex depends on the impurity–vacancy distance (the nearest or distant vacancy) [4, 5].

Recent experiments have shown that SrTiO₃ doped with cobalt with a concentration of 14–40% is a ferromagnet at 300 K and, at the same time, a dielectric [6, 7], which is a rather rare combination. This was one of the reasons for the present study. The preliminary study of

this material suggested a possible incorporation of the Co impurity into different sites of the perovskite structure [8].

Cobalt-doped strontium titanate has been studied for a rather long time. The similarity of the crystal structures of SrTiO₃ and SrCoO_{3–*x*} (oxygen-deficient perovskite) suggests the existence of a continuous series of solid solutions in this system. According to Ref. [9], the solubility of cobalt at the *B* site of SrTiO₃ is at least 40%, whereas the authors [10] reported the preparation of polycrystalline samples containing up to 90% of Co using the solid-phase synthesis. The X-ray studies performed in [10] revealed the appearance of additional peaks in X-ray diffraction patterns at $x > 0.5$; these peaks were associated with the oxygen vacancies ordering. In all earlier published papers, it was presumed that the cobalt atom substitutes the titanium one. No information about the incorporation of cobalt into the *A* site has been reported.

The oxidation state of cobalt in SrTiO₃(Co) was determined by electron paramagnetic resonance (EPR), X-ray photoelectron spectroscopy (XPS), optical absorption, and X-ray absorption near-edge structure (XANES) spectroscopy. According to the EPR data [11], a signal from Co⁴⁺ ions in a low-spin state ($S = 1/2$) was observed in single crystals doped with 0.2% Co, and the signal intensity strongly increased after preliminary illumination. It seems that the cobalt impurity in this sample is diamagnetic in the initial state and is in the +3 oxidation state. Indeed, the studies of the optical absorption spectra of single crystals [11, 12] have revealed the absorption lines typical of the Co³⁺ ion in an octahedral environment. The XPS studies of thin films grown by molecular-beam epitaxy (MBE) at 550°C with a cobalt concentration from 10 to 50% [7] brought to a conclusion that the cobalt oxidation state is 2+. The conclusion about the same oxidation state was also made from XPS studies of SrTiO₃(Co) nanofibers, which had a cobalt concentration up to 20% and were prepared by electrospinning and annealed at 650°C [13], and of the samples with 30% Co grown by pulsed laser deposition (PLD) [6]. The analysis of XPS data enabled the au-

* irinasluch@gmail.com

thors [6] to suppose that the impurity Co atoms replace Ti ions with the formation of oxygen vacancies, and the oxidation state of cobalt in films is lower than in bulk samples, as the films were grown at a low partial pressure of oxygen. (Since the oxidation state of cobalt at the *B* site differs from the titanium ion charge, this implies the existence of compensating defects in the samples, in particular, oxygen vacancies.)

It should be noted that as the spread of photoelectron peak energies for the Co atom exceeds their chemical shift upon a change in the oxidation state [14], the conclusion [6, 7] about its 2+ oxidation state in SrTiO₃ was made from the appearance of a strong high-energy satellite peak. However, the same peak with a slightly lower intensity is also present in the samples with trivalent cobalt [15], so the reliability of this oxidation state determination method is questionable. An indirect argument for the appearance of Co²⁺ in films synthesized by PLD may be an increase in the out-of-plane lattice constant with increasing cobalt concentration [6]. This effect obviously differs from the decrease in the lattice constant observed when doping the bulk crystals [10, 16]. Unfortunately, no conclusions about the oxidation state of cobalt have been drawn from the XANES spectra recorded on SrTiO₃(Co) films [6].

To explain the origin of the room-temperature ferromagnetism, a number of theoretical studies [7, 17, 18], in which the nature of this phenomenon was discussed assuming the presence of divalent cobalt in the samples, have been performed. These studies have demonstrated an essential role of oxygen vacancies, which form Co²⁺ ion-nearest vacancy complexes with a nonzero magnetic moment.

The studies of the magnetic properties of cobalt-doped SrTiO₃ samples have shown that the bulk synthesis methods do not usually result in the appearance of ferromagnetism at room temperature [10, 16]. Instead, a quite different paramagnetic-antiferromagnetic phase transition was observed in single-phase SrTi_{1-x}Co_xO₃ samples with $x = 0.35-0.50$ at 15–26 K [16]. The X-ray diffraction studies of these samples reduced in a 10% H₂-Ar atmosphere revealed the presence of metallic Co in them. In contrast, thin cobalt-doped SrTiO₃ films grown by the PLD or MBE methods with dielectric or semiconducting properties exhibit ferromagnetism at 300 K at a high impurity concentration (>14%) [6, 7, 19]. Cobalt-doped thin (La,Sr)TiO₃ films, which were annealed in a reducing atmosphere and had metallic conductivity, demonstrate ferromagnetism at 300 K at a much lower cobalt content (~2%) [20, 21].

It should be noted that the properties of samples strongly depend on the method of their preparation. The samples prepared at high temperatures are characterized by the presence of trivalent cobalt and the absence of ferromagnetism. On the contrary, divalent cobalt and ferromagnetism at 300 K appear under conditions, which can be considered as far from equilibrium (hydrothermal synthesis, PLD, nanofibers). This makes the problem of

determining the real structure of impurity defects formed by cobalt very topical.

In this work, the structural position and oxidation state of magnetic Co impurity in SrTiO₃ samples prepared by solid-phase synthesis with different deviations from stoichiometry are studied by XAFS spectroscopy. It is shown that, depending on the preparation conditions, the cobalt atoms can predominantly enter either the *B* sites of the perovskite structure in the trivalent state, or the *A* sites in the divalent state. In the latter case, the impurity is off-center and is in the high-spin state. The obtained results are compared with the results of the first-principles calculations of the defect structure.

II. SAMPLES, EXPERIMENTAL AND CALCULATION TECHNIQUES

Cobalt-doped SrTiO₃ samples with an impurity concentration of 2–3% and different deviations from stoichiometry were prepared by solid-phase synthesis. The initial components were SrCO₃, nanocrystalline TiO₂ synthesized by the hydrolysis of tetrapropylorthotitanate and dried at 500°C, and Co(NO₃)₂·6H₂O. The components were weighed in required proportions, ground in acetone, and annealed in air in alumina crucibles at 1100°C for 4 h. The resulting powders were ground again and repeatedly annealed under the same conditions for 4 h. Some samples were additionally annealed in air at 1500 or 1600°C for 2 h. To incorporate cobalt into the *A* or *B* site of the perovskite structure, the composition of the samples was deliberately deviated from stoichiometry towards excess titanium or strontium. All the prepared samples were dark brown in color.

Extended X-ray absorption fine structure (EXAFS) and X-ray absorption near-edge structure (XANES) spectra were recorded in fluorescence mode at the Co *K*-edge (7.709 keV) and 300 K on the KMC-2 station of the BESSY synchrotron radiation source (Germany). Radiation was monochromatized with a double-crystal Si_{1-x}Ge_x (111)-oriented monochromator. The intensity of radiation incident on a sample was measured with an ionization chamber, whereas the intensity of the fluorescence radiation was measured with a RÖNTEC energy-dispersive silicon drift detector.

The EXAFS spectra were analyzed with a widely used IFEFFIT software package [22]. The EXAFS function $\chi(k)$ (here, $k = \sqrt{2m(E - E_0)}/\hbar$ is the wave vector of a photoelectron and E_0 is the absorption edge energy) was extracted from the experimental spectra using the ATHENA software and fitted with the ARTEMIS software to the theoretical curve calculated for a chosen structural model

$$\chi(k) = -\frac{1}{k} \sum_j \frac{N_j S_0^2}{R_j^2} |f_j(k)| \times \exp[-2\sigma_j^2 k^2 - 2R_j/\lambda(k)] \sin[2kR_j + \phi_j(k)], \quad (1)$$

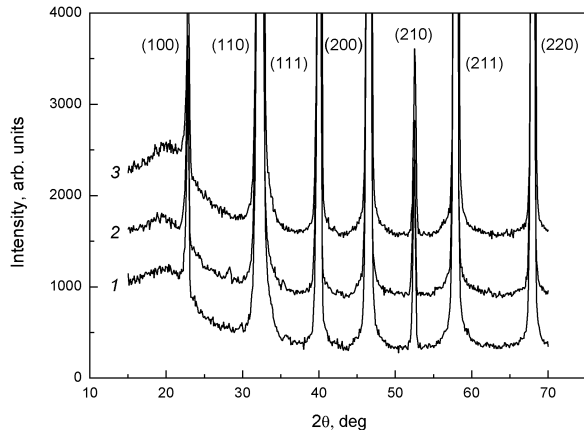


FIG. 1. X-ray diffraction patterns for the samples (1) $\text{Sr}_{0.98}\text{Co}_{0.02}\text{TiO}_3$ annealed at 1600°C , (2) $\text{Sr}_{0.98}\text{Co}_{0.02}\text{TiO}_3$ annealed at 1500°C , (3) $\text{SrTi}_{0.97}\text{Co}_{0.03}\text{O}_3$ annealed at 1500°C .

where the sum runs over several nearest shells j about the central Co atom, N_j is the number of atoms in the j th coordination shell, R_j is its radius, f_j is the scattering amplitude, λ is an effective mean free path, σ_j^2 is the Debye–Waller factor characterizing the mean-squared deviation between the distance to atoms of the j th sort from its mean value, and S_0^2 is the multiplier taking into account the reduction in the oscillation amplitude resulting from many-body effects. The scattering amplitude $f_j(k)$, the phase shifts $\phi_j(k)$, and the mean free path $\lambda(k)$ for all single- and multiple-scattering paths were calculated using the FEFF6 software. For each sample, 3–4 spectra were recorded and further independently processed, and the obtained curves $\chi(k)$ were averaged. The details of the data analysis are given in [23].

The first-principles calculations of the geometry and magnetic and electronic structures of impurity centers were performed using the ABINIT software within the LDA+ U approach on 80-atom cubic supercells, in which one of the Ti^{4+} ions at the B site or one of the Sr^{2+} ions at the A site of the perovskite structure was substituted by the cobalt ion. The atoms with partially filled d shell were described using the projector-augmented wave (PAW) pseudopotentials. The parameters describing the Coulomb and exchange interactions inside the d shell were $U = 5$ and $J = 0.9$ eV.

III. EXPERIMENTAL RESULTS

The X-ray diffraction analysis of prepared samples showed that all studied $\text{SrTiO}_3(\text{Co})$ samples were single-phase and had a cubic perovskite structure at 300 K. Typical X-ray diffraction patterns of three samples are shown in Fig. 1, and their unit cell parameters together with the unit cell parameter of undoped SrTiO_3 are given

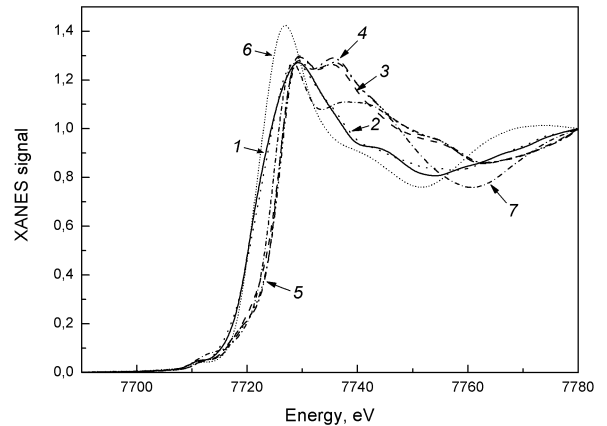


FIG. 2. XANES spectra for $\text{SrTiO}_3(\text{Co})$ samples and reference cobalt compounds: (1) $\text{Sr}_{0.98}\text{Co}_{0.02}\text{TiO}_3$ annealed at 1600°C , (2) $\text{Sr}_{0.98}\text{Co}_{0.02}\text{TiO}_3$ annealed at 1500°C , (3) $\text{Sr}_{0.98}\text{Co}_{0.02}\text{TiO}_3$ annealed at 1100°C , (4) $\text{SrTi}_{0.97}\text{Co}_{0.03}\text{O}_3$ annealed at 1500°C , (5) $\text{SrTi}_{0.97}\text{Co}_{0.03}\text{O}_3$ annealed at 1100°C , (6) $\text{Co}(\text{NO}_3)_2 \cdot 6\text{H}_2\text{O}$, (7) LaCoO_3 .

in Table I. A decrease in the unit cell parameter of all doped specimens in comparison with undoped SrTiO_3 agrees with the earlier published data [10, 16] and indicates the formation of a solid solution.

The oxidation state of the Co impurity in doped SrTiO_3 samples was determined by comparing the absorption edge position in the XANES spectra of the samples with the edges positions in the reference samples LaCoO_3 (cobalt valence +3) and $\text{Co}(\text{NO}_3)_2 \cdot 6\text{H}_2\text{O}$ (cobalt valence +2). The XANES spectra of all samples and reference compounds are shown in Fig. 2.

The comparison of the XANES spectra of all $\text{SrTiO}_3(\text{Co})$ samples annealed at a temperature of 1100°C and the sample annealed at 1500°C with deviation from stoichiometry towards excess strontium showed that the absorption edges in these samples are close to each other and almost coincide with the absorption edge of the LaCoO_3 reference compound. This suggests that the Co impurity in these samples is predominantly in the +3 oxidation state.

The absorption edges of $\text{SrTiO}_3(\text{Co})$ samples annealed at 1500 and 1600°C with deviation from stoichiometry towards excess Ti coincide with each other and are close to the absorption edge of the $\text{Co}(\text{NO}_3)_2 \cdot 6\text{H}_2\text{O}$ reference compound. This indicates that these samples contain cobalt predominantly in the +2 oxidation state.

It should be noted that the chemical shift in the XANES spectra is much larger than that in the photoelectron spectra [14], thus providing the possibility to make a more reliable conclusion about the oxidation state of cobalt.

To determine the structural position of the Co impurity in SrTiO_3 , the EXAFS spectra were analyzed.

TABLE I. Unit cell parameters for three SrTiO₃(Co) samples and undoped SrTiO₃

Sample	Sr _{0.98} Co _{0.02} TiO ₃ annealed at 1600°C	Sr _{0.98} Co _{0.02} TiO ₃ annealed at 1500°C	SrTi _{0.97} Co _{0.03} O ₃ annealed at 1500°C	SrTiO ₃
Unit cell parameter a (Å)	3.8977±0.0005	3.8994±0.0002	3.8931±0.0006	3.905

The data analysis and the choice of a structural model were performed taking into account the results of X-ray diffraction and XANES studies, namely, the unit cell parameter and the ability of Co atoms to enter different (A and B) sites of the perovskite structure, probably simultaneously and in different oxidation states.

The comparison of EXAFS spectra for two groups of samples, in which Co ions are in different oxidation states, reveals a qualitative distinction between them.

For all samples in which Co is in the Co³⁺ oxidation state, a reasonable agreement between the experimental spectra and the theoretically calculated curves $\chi(k)$ was obtained for the model, in which the Co³⁺ ion substitutes the Ti⁴⁺ ion with the formation of a distant oxygen vacancy. In this model, the Co–O distance in the first shell was 1.909 ± 0.012 Å, the Co–Sr distance was 3.342 ± 0.016 Å, and the Co–Ti distance was 3.892 ± 0.012 Å.

The analysis of EXAFS spectra for the Sr_{0.98}Co_{0.02}TiO₃ samples annealed at 1600 and 1500°C, in which the impurity Co atom is in the +2 oxidation state, has shown that none of the models, in which the Co²⁺ ion substitutes either Ti⁴⁺ at the B site or Sr²⁺ at the A site, agree satisfactorily with the experiment. Qualitative agreement between the experimental spectrum and the theoretically calculated EXAFS curve for these samples was obtained for the model, in which the Co²⁺ ion replaces the Sr²⁺ ion at the A site and is displaced from this site in the [100] direction by ~ 1.0 Å. This displacement seems to be reasonable taking into account a large difference between the Co²⁺ and Sr²⁺ ionic radii. In this case, the distance from the cobalt atom to the nearest oxygen atoms is 1.993 ± 0.042 Å.

Unfortunately, the agreement between the experimental and theoretically calculated EXAFS curves was not sufficiently good for all studied samples (the criterion of agreement between the calculated and experimental spectra was a low R -factor, the correspondence of obtained coordination numbers to the theoretical model, and the agreement between the Fourier transforms of spectra in the R -representation). For this reason, it was decided to consider the microscopic models of different impurity centers with the Co atom at the A and B sites.

IV. RESULTS OF FIRST-PRINCIPLES CALCULATIONS

The construction of theoretical models was performed taking into account the data on the oxidation state of impurity atoms and the interatomic distances obtained from

the analysis of EXAFS spectra. We note that the earlier first-principles calculations [7, 17, 18] were performed mainly for the divalent cobalt at the B site, while our results indicate other oxidation states and lattice sites.

The modeling of the geometry of impurity centers was started from the Co²⁺ ion at the A site. This impurity center is one of the simplest ones, as the substitution of strontium by cobalt does not require any charge compensation. The calculations, which took into account the full relaxation of the local environment, showed that the on-center position of the Co²⁺ ion at the A site in SrTiO₃ is energetically unstable, and the impurity atom displaces to an off-center position. The comparison of the energies of structures with atoms displaced along the [100], [110], and [111] directions showed that the structure with the displacement along the [110] axis has the lowest energy, and the energy of the structures with the displacements along the [100] and [111] axes are, respectively, by 264 and 985 meV (per Co atom) higher. The displacements along the [100], [110], and [111] axes are 1.03, 1.00, and 0.79 Å, respectively, and the ion magnetic moment is $S = 3/2$ in all configurations. The calculated distances to the nearest atoms in the cobalt environment for these configurations are given in Table II. It is seen that the calculated distances to the nearest oxygen atoms appreciably exceed the Co–O distances for cobalt at the B site, and the interatomic distances for the displacements along the [100] and [111] axes are closest to the experimentally obtained value of 1.993 ± 0.042 Å.

The modeling of impurity centers with trivalent cobalt at the B site implies the existence of defects compensating the difference between the ionic charges. The calculations for an isolated Co³⁺ ion at the B site, for which an additional electron was provided by a distant F donor atom located at the oxygen site (Table II), have shown that the low-spin state ($S = 0$) has the lowest energy. The comparison of the distances obtained in the model, in which the Co³⁺ ion enters the B site, with the experimentally determined distance of 1.909 ± 0.012 Å shows their good agreement.

The electronic structure of the Co²⁺ impurity center at the A site is shown in Fig. 3(a). It is seen that the cobalt impurity creates three acceptor levels associated with the occupied $d_{x^2-y^2}$ (spin up) and d_{z^2} and d_{xy} (spin down) orbitals in the forbidden gap of SrTiO₃. The Fermi level F is located in the forbidden gap. The d_{z^2} state is strongly hybridized with the oxygen p states, so the optical transitions allowed by the selection rules from this level to the bottom E_c of the conduction band (which is formed by cobalt and titanium d states) may be the cause of intense color of the samples.

TABLE II. Local environment of Co ions in different theoretical models. The distances are in Å.

Model	S	Shell					
		1	2	3	4	5	6
Off-center atom at the A site, displacement [100]	3/2	2.014	2.948	3.056	3.168	3.630	3.814
		(4O)	(4Ti)	(1Sr)	(4O)	(4O)	(4O)
Off-center atom at the A site, displacement [110]	3/2	2.051	2.069	2.706	3.265	3.318	3.474
		(1O)	(4O)	(2Ti)	(2O)	(2Sr)	(4Ti)
Off-center atom at the A site, displacement [111]	3/2	1.996	2.707	2.946	3.216	3.523	3.564
		(3O)	(1Ti)	(6O)	(3Ti)	(3Sr)	(3O)
Isolated Co^{3+} ion at the B site	0	1.905	3.352	3.801	4.355	5.509	
		(6O)	(8Sr)	(6Ti)	(24O)	(12Ti)	

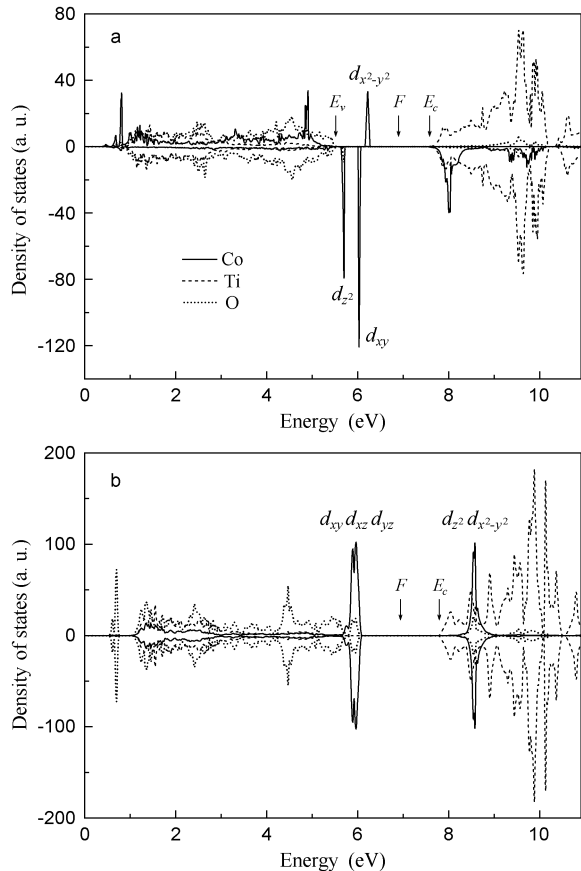


FIG. 3. Partial contributions of cobalt, titanium, and oxygen to the density of states for (a) Co_A^{2+} and (b) Co_B^{3+} impurity centers. Partial contribution of cobalt was decreased by 5 times.

For an isolated Co^{3+} impurity center at the B site, the cobalt d levels of T_{2g} symmetry merge together with the valence band edge, whereas the levels of E_g symmetry form resonant levels in the conduction band (Fig. 3(b)). That is why there are no reasons to expect appreciable change in the color of samples in this case.

V. REFINEMENT OF THE STRUCTURAL MODELS AND DISCUSSION OF RESULTS

Insufficiently good agreement obtained between the experimental and calculated EXAFS spectra in Sec. III has stimulated us to consider more complicated models. First, we considered the model, in which cobalt at the B site forms a complex with the nearest oxygen vacancy. The distances obtained in this model for the $\text{SrTi}_{0.97}\text{Co}_{0.03}\text{O}_3$ sample annealed at 1100°C are only slightly different from the values given above, but the parameter S_0^2 was closer to its value for the reference compounds.

Using the geometry of the local environment of the off-center cobalt atom at the A site calculated for three directions of displacement, the spectrum of the $\text{Sr}_{0.98}\text{Co}_{0.02}\text{TiO}_3$ sample annealed at 1600°C was processed. It turned out that the lowest R factor is obtained by fitting curves for configurations with the [100] and [111] displacements. The calculated Fourier transform of the EXAFS spectrum for the model with the [110] displacement had a strong peak from Ti atoms in the third shell, but this peak was entirely absent in the experimental spectrum. For this reason, the [110] displacement may be completely excluded from further consideration. Taking into account an appreciable difference in energy between the configurations with the [100] and [111] displacements, we believe that the displacement of atoms occurs in the [100] direction and shall consider only this model in what follows.

Further, we have supposed that cobalt atoms in actual samples may substitute atoms at the A and B sites simultaneously. The structural parameters for two EXAFS spectrum components, which will be called states A and B and in which the impurity atoms substitute the corresponding lattice sites, were determined as follows. As a starting point, it was assumed that the spectrum of the $\text{SrTi}_{0.97}\text{Co}_{0.03}\text{O}_3$ sample annealed at 1100°C represents the spectrum of “pure” state B . The local environment of cobalt at the B site was modeled taking into account the nearest oxygen vacancy. For this model, a set of structural parameters (distances and Debye–Waller factors for three nearest shells) was calculated. The spec-

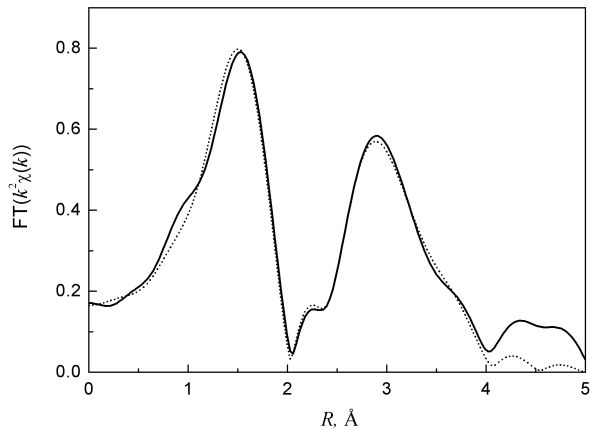


FIG. 4. Comparison of Fourier transform amplitudes for a typical EXAFS spectrum of the $\text{Sr}_{0.98}\text{Co}_{0.02}\text{TiO}_3$ sample annealed at 1600°C (solid line) with the calculated curve (dotted line) corresponding to the best fit.

trum of the $\text{Sr}_{0.98}\text{Co}_{0.02}\text{TiO}_3$ sample annealed at 1600°C was then presented as a sum of states A and B with unknown relative fractions. Fixing the parameters determined for state B at the previous step and taking the interatomic distances predicted by first-principles calculations for state A (see Sec. IV) as another starting point, we estimated the structural parameters for state A and the relative fractions of states A and B . Further, assuming that the $\text{SrTi}_{0.97}\text{Co}_{0.03}\text{O}_3$ sample annealed at 1100°C may contain a small fraction of state A , we performed a new analysis of the EXAFS spectrum of this sample. At this step, the data obtained for state A at the previous step were fixed. This gave the refined parameters for state B and the relative fractions of states A and B in this sample. The multiple repetition of the described iterative procedure provided the structural parameters for states A and B and their relative fractions in the analyzed spectra.

A typical experimental EXAFS spectrum and its best theoretical fit within the described approach are shown in Fig. 4, and the interatomic distances to the nearest shells for samples annealed at 1100 and 1600°C are given in Table III. The interatomic distances obtained from experiment agree with their calculated values (compare Tables II and III). According to the iterative procedure results, the $\text{Sr}_{0.98}\text{Co}_{0.02}\text{TiO}_3$ sample annealed at 1600°C contains 76% of the incorporated cobalt at the A site, whereas the $\text{SrTi}_{0.97}\text{Co}_{0.03}\text{O}_3$ sample annealed at 1100°C contains nearly 18% of impurity atoms at the A site.

VI. CONCLUSIONS

In this paper, the results of XAFS spectroscopy study of the local structure and oxidation state of the cobalt impurity in SrTiO_3 have been considered. It was revealed that under certain synthesis conditions cobalt may be incorporated into the A site of the perovskite structure. By varying the synthesis conditions, it is possible to appreciably change the ratio of concentrations of cobalt atoms incorporated into the A and B sites. Thus, 76% of Co atoms enter the A site at an annealing temperature of 1600°C and only 18% of them enter this site at 1100°C .

The study of XANES spectra showed that the oxidation state of cobalt is $+2$ at the A site and $+3$ at the B site. It was established that the absorption edge shift in the XANES spectra is much more sensitive to the change in the oxidation state of cobalt in comparison with XPS. EXAFS studies revealed that Co atoms at the A site are off-center, and their displacement is ~ 1.0 Å. According to first-principles calculations, the magnetic moment of the Co_A^{2+} ion is $S = 3/2$. Thus, Co_A^{2+} ions in SrTiO_3 are another representative of the group of magnetic off-center impurities, with which interesting multi-ferroic properties may be associated.

ACKNOWLEDGMENTS

This work was supported by the Russian Foundation for Basic Research (grant no. 17-02-01068).

-
- [1] V. V. Shvartsman, S. Bedanta, P. Borisov, W. Kleemann, A. Tkach, and P. M. Vilarinho, *Phys. Rev. Lett.* **101**, 165704 (2008).
 - [2] A. I. Lebedev, I. A. Sluchinskaya, A. Erko, and V. F. Kozlovskii, *JETP Lett.* **89**, 457 (2009).
 - [3] I. A. Sluchinskaya, A. I. Lebedev, and A. Erko, *Bull. Russ. Acad. Sci.: Phys.* **74**, 1235 (2010).
 - [4] I. A. Sluchinskaya, A. I. Lebedev, and A. Erko, *J. Adv. Dielectrics* **3**, 1350031 (2013).
 - [5] I. A. Sluchinskaya, A. I. Lebedev, and A. Erko, *Phys. Solid State* **56**, 449 (2014).
 - [6] L. Bi, H.-S. Kim, G. F. Dionne, and C. A. Ross, *New J. Phys.* **12**, 043044 (2010).
 - [7] A. B. Posadas, C. Mitra, C. Lin, A. Dhamdhere, D. J. Smith, M. Tsoi, and A. A. Demkov, *Phys. Rev. B* **87**, 144422 (2013).
 - [8] A. I. Lebedev and I. A. Sluchinskaya, in *Fundamental Physics of Ferroelectrics and Related Materials, Proceedings of the 2016 Workshop* (2016) pp. 211–212.
 - [9] A. Murashkina, V. Maragou, D. Medvedev, V. Sergeeva, A. Demin, and P. Tsiakaras, *J. Power Sources* **210**, 339 (2012).
 - [10] S. Malo and A. Maignan, *Inorg. Chem.* **43**, 8169 (2004).
 - [11] K. W. Blazey and K. A. Muller, *J. Phys. C: Solid State Physics* **16**, 5491 (1983).
 - [12] Y. Doichilovich, N. Kulagin, D. Popovich, and S. Spasov

TABLE III. Structural parameters determined from the EXAFS spectra analysis of two studied samples

Sample	Model	R -factor	S_0^2	Shell	R_i (Å)	σ_i^2 (Å ²)
Sr _{0.98} Co _{0.02} TiO ₃ annealed at 1600°C	Site <i>A</i>	0.00297	0.705	$R_{\text{Co-O}}$	2.040(6)	0.0049(18)
				$R_{\text{Co-Ti}}$	3.094(15)	0.0146(27)
				$R_{\text{Co-Sr}}$	2.816(20)	0.0114(40)
	Site <i>B</i>	0.282	$R_{\text{Co-O}}$	1.906(11)	0.0037(18)	
			$R_{\text{Co-Sr}}$	3.354(19)	0.0087(12)	
			$R_{\text{Co-Ti}}$	3.907(17)	0.0064(13)	
SrTi _{0.97} Co _{0.03} O ₃ annealed at 1100°C	Site <i>A</i>	0.00255	0.153	$R_{\text{Co-O}}$	2.040(6)	0.0049(18)
				$R_{\text{Co-Ti}}$	3.094(15)	0.0146(27)
				$R_{\text{Co-Sr}}$	2.816(20)	0.0114(40)
	Site <i>B</i>	0.731	$R_{\text{Co-O}}$	1.906(11)	0.0037(18)	
			$R_{\text{Co-Sr}}$	3.354(19)	0.0087(12)	
			$R_{\text{Co-Ti}}$	3.907(17)	0.0064(13)	

vich, Cryst. Reports **49**, 469 (2004).

- [13] W. Zhang, H.-P. Li, and W. Pan, J. Mater. Sci. **47**, 8216 (2012).
- [14] “NIST x-ray photoelectron spectroscopy database,” <http://srdata.nist.gov/>.
- [15] A. Chainani, M. Mathew, and D. D. Sarma, Phys. Rev. B **46**, 9976 (1992).
- [16] C. Pascanut, N. Dragoie, and P. Berthet, J. Magn. Magn. Mater. **305**, 6 (2006).
- [17] J. M. Florez, S. P. Ong, M. C. Onbaşlı, G. F. Dionne, P. Vargas, G. Ceder, and C. A. Ross, Appl. Phys. Lett. **100**, 252904 (2012).
- [18] C. Mitra, C. Lin, A. B. Posadas, and A. A. Demkov, Phys. Rev. B **90**, 125130 (2014).
- [19] S. X. Zhang, S. B. Ogale, D. C. Kundaliya, L. F. Fu, N. D. Browning, S. Dhar, W. Ramadan, J. S. Higgins, R. L. Greene, and T. Venkatesan, Appl. Phys. Lett. **89**, 012501 (2006).
- [20] Y. G. Zhao, S. R. Shinde, S. B. Ogale, J. Higgins, R. J. Choudhary, V. N. Kulkarni, R. L. Greene, T. Venkatesan, S. E. Lofland, C. Lanci, J. P. Buban, N. D. Browning, S. Das Sarma, and A. J. Millis, Appl. Phys. Lett. **83**, 2199 (2003).
- [21] G. Herranz, R. Ranchal, M. Bibes, H. Jaffrès, E. Jacquet, J.-L. Maurice, K. Bouzehouane, F. Wyczisk, E. Tafrá, M. Basletic, A. Hamzic, C. Colliex, J.-P. Contour, A. Barthélémy, and A. Fert, Phys. Rev. Lett. **96**, 027207 (2006).
- [22] “Ifeffit project home page,” <http://cars.uchicago.edu/ifeffit/>.
- [23] A. I. Lebedev, I. A. Sluchinskaya, V. N. Demin, and I. H. Munro, Phys. Rev. B **55**, 14770 (1997).